Root litter decomposition slows with soil depth

Caitlin E. Hicks Pries[1,2], Benjamin N. Sulman[3,4], Corinna West[5], Caitlin O'Neill[6], Erik Poppleton[7,8], Rachel C. Porras[2], Cristina Castanha[2], Biao Zhu[9], Daniel B. Wiedemeier[10], and Margaret S. Torn[2]

[1]Department of Biological Sciences, Dartmouth College, Hanover, NH
[2]Climate and Ecosystem Science Division, Earth and Environmental Science Area, Lawrence Berkeley National Laboratory, Berkeley, CA
[3]Program in Atmospheric and Oceanic Sciences, Princeton University, Princeton, NJ
[4]Sierra Nevada Research Institute, University of California, Merced, CA
[5]Department of Curriculum and Instruction, University of Wisconsin—Madison, Madison, WI
[6]Department of Plant Biology, University of Illinois at Urbana-Champaign, Urbana, IL
[7]Biological Design Institute, Arizona State University, Tempe, AZ
[8]Department of Biology, Tufts University, Medford, MA
[9]Institute of Ecology, College of Urban and Environmental Sciences, and Key Laboratory for Earth Surface Processes of the Ministry of Education, Peking University, Beijing, China
[10]Department of Geography, University of Zurich, Zurich, Switzerland
*corresponding author: caitlin.e.h.pries@dartmouth.edu, 603-646-2052

Abstract

Even though over half of the world's soil organic carbon (SOC) is stored in subsoils (>20 cm deep), and the old ages of subsoil OC indicate its cycling differs from surface SOC, there are few studies examining in situ decomposition processes in deep soils. Here, we added ^{13}C-labeled fine roots to 15, 55, and 95 cm depths of a well-characterized coniferous forest Alfisol and monitored the amount of root-derived C remaining over 6, 12, and 30 months. We recovered the root-derived C in microbial phospholipid fatty acids (PLFAs) after 6 months and in coarse (>2 mm) particulate, fine (<2 mm) particulate, and dense, mineral-associated pools after 6, 12, and 30 months. Overall, root decomposition in the first 6 months was similar among all depths but significantly diverged at 30 months with faster decomposition at 15 cm than at 95 cm. There were more fungal and Gram negative-associated PLFAs at 15 cm than at 95 cm, and ^{13}C analysis revealed those microbial groups preferred the added root carbon to native SOC. Mineral-associations were not the cause of slower decomposition at depth because similar amounts of applied root C was recovered in the dense fraction at all depths. The largest difference among depths was in the amount of root C recovered in the coarse particulate fraction, which was greater at 95 cm (50%) than at 15 cm (15%). Slower decomposition of the particulate pool at depth likely contributed to the increase in C:N ratios and depletion of δ^{13}C values below 60 cm depth in our soil profiles. Simulations of these soils using the CORPSE model, which incorporates microbial priming effects and mineral stabilization of SOC, reproduced patterns of particulate and mineral-associated SOC over both time and depth and suggested that a lack of priming by root exudates at depth could account for the slower decomposition rate of particulate root material.

Decomposition of deep particulate SOC may increase if root exudation or dissolved OC transport at depth increases.

Keywords: Soil organic matter, carbon, decomposition, soil depth, 13C, fine root, density fractionation, PLFA

Highlights

- Fine root decay was similar across depths at first but then stalled at 95 cm
- Organo-mineral associations were not the cause of slower decomposition at depth
- Fine root litter at depth was stuck in the coarse particulate fraction
- The CORPSE model showed how a lack of root exudates could slow decay at depth

Introduction

Understanding how decomposition changes with depth is integral to understanding the capacity of deeper soils to store SOC and how vulnerable deeper SOC stocks are to loss due to global change. For instance, if decomposition rates are slower at depth than the surface due to a lack of fresh substrates, then increased plant allocation to roots or shifts in plant community to more deeply-rooted species may increase decomposition. On the other hand, if decomposition rates at depth are slower due to increased mineral associations or physical protection, SOC stored at depth may be resistant to losses due to global changes like shifting plant communities or warming. However, the processes controlling the cycling of deep SOC have received little attention even though over half of the world's soil organic carbon (SOC) pool is stored below 20 cm (Jobbágy and Jackson, 2000) and long turnover times of deep SOC (Mathieu et al., 2015) imply processes at depth differ from those in the surface soil.

SOC cycling changes with depth because the soil profile is a gradient of interacting biotic and abiotic factors. The majority of plant inputs in the forms of shoot litter, senescent roots, and root exudates are found in the surface soil (<20 cm; Jobbágy and Jackson, 2000; Schrumpf et al., 2013). The lack of inputs to prime microbial activity, such as dissolved organic matter from root exudates or leached litter, can slow decomposition in the subsurface (Fontaine et al., 2007; Kuzyakov, 2010) due to energy (Salomé et al., 2010) or nutrient limitation (Heitkötter et al., 2017). With increasing depth, microbial biomass decreases, and community composition becomes less diverse (Eilers et al., 2012; Fierer et al., 2003; Kramer and Gleixner, 2008). Surface soils also contain more eukaryotes, like fungi (Fierer et al., 2003), arthropods (Petersen and

83 Luxton, 1982), and earthworms (Jiménez and Decaëns, 2000; Lavelle, 1988), which play
84 active roles in bioturbation (Lavelle et al., 2006; Six et al., 2004). At depth, with reduced
85 C inputs and less abundant biota, the influence of soil minerals predominates, leading to a
86 larger proportion of SOM being mineral-associated at depth than at the surface (Angst et
87 al., 2016; Kögel-Knabner et al., 2008; Rumpel et al., 2002; Schrumpf et al., 2013).
88 Microbes compete with mineral sorption sites for SOC, so mineral type, charge, and
89 reactive surface area become important controls on SOM stabilization. At depth,
90 decomposition can also be limited by the physical disconnection between microbes and
91 SOC caused by spatial heterogeneity (Gleixner, 2013; Heinze et al., 2018).
92 Compared to the research on surface litter decomposition, few studies have
93 examined how decomposition of plant litter changes with depth in situ (e.g., Bird and
94 Torn, 2006; Gill and Burke, 2002; Solly et al., 2015), and even fewer have examined
95 decomposition throughout the top meter of the soil profile (e.g., Gill and Burke, 2002;
96 Preusser et al., 2017; Sanaullah et al., 2011). Results from these studies have shown that
97 in situ decomposition rates are initially similar across depths. However, Hicks Pries et al.
98 (2017a) recently showed that decomposition, particularly of the <2 mm soil fraction,
99 slowed in the A horizon relative to the O horizon between the fifth and tenth years of
100 decay, likely as a result of organo-mineral associations. Similarly, a litter bag study of
101 root decomposition found that mass loss rates declined linearly from 10 to 100 cm (Gill
102 and Burke, 2002).
103 Similar to results tracking the loss of fresh litter inputs in situ, results from
104 incubations that measured how the respiration of SOC changes with depth have been
105 equivocal. When carbon losses are normalized by SOC content, incubations have shown

similar decomposition rates across depths (Salomé et al., 2010), faster decomposition rates in deeper soils (Wordell-Dietrich et al., 2017), and slower decomposition rates in deeper soils (Gabriel and Kellman, 2014; Gillabel et al., 2010). In one incubation study, sieving increased respiration rates from subsoils but not from surface soils, implying SOC at depth was either protected in aggregates or physically separated from microbes (Salomé et al., 2010). Other incubation studies have shown positive priming effects with the addition of glucose (Karhu et al., 2016), cellulose (Fontaine et al., 2007), or organic acids (Heitkötter et al., 2017) in deeper soils, indicating that decomposition at depth is energy-limited.

The processes behind declines in SOC turnover rates with depth have not been explicitly included in most SOC modeling studies. While past modeling studies have included a decline in SOC turnover rate as a function of depth, this was typically done using empirical parameterization rather than a process-based approach (e.g., Jenkinson and Coleman, 2008; Koven et al., 2013). Koven et al. (2013) speculated that this pattern could be due to oxygen availability or priming effects but did not explicitly simulate these processes. Recent developments in explicitly modeling microbial decomposition and organo-mineral interactions (e.g., Sulman et al., 2014) now allow us to explicitly simulate interactions between C inputs and microbial growth. We can use these tools to investigate the extent to which stimulation of microbial activity by fresh C inputs near the surface and mineral stabilization of SOC at depth can explain observed declines in SOC turnover with depth. By evaluating these new models in the context of observations, we can move toward placing biogeochemical modeling of subsoils on a firmer mechanistic foundation.

Here, we incubated ^{13}C-labeled roots in situ at three depths (15, 55, and 95 cm) of a coniferous forest Alfisol over 2.5 years. We wanted to understand how the decomposition process changes with soil depth including C mineralization, biological assimilation by microbes, and transformation of litter C into SOC. Our specific objectives were to 1) quantify differences in total retention and transformations of root litter into fine particulate and mineral-associated organic matter among depths; 2) explore whether patterns in the soil profile explain root decomposition differences and how root decomposition differences may explain observed SOC patterns with depth; 3) investigate how the abundance of microbial groups and their use of the root litter differed with depth using ^{13}C-specific phospholipid fatty acid analysis; 4) use an SOC decomposition model with explicit representation of microbial decomposition and SOC-mineral interactions (Sulman et al., 2014) to test whether microbial responses to root exudates could explain decomposition differences across depths.

Methods

Study Site

The University of California Blodgett Experimental Forest is located in the foothills of the Sierra Nevada near Georgetown, CA at 120°39'40"W; 38°54'43"N at 1370 m above sea level and below the permanent winter snowline. Mean annual precipitation is 1774 mm, with most of it occurring from November through April. Mean annual temperature is about 12.5°C (Bird and Torn, 2006). The decomposition experiment was in a thinned 80-year-old stand of mixed conifers including ponderosa pine (*Pinus ponderosa*), sugar pine (*Pinus lambertiana*), incense cedar (*Calodefrus decurrens*), white fir (*Abies concolor*), and douglas fir (*Pseudotsuga menziesii*). The soils are Holland series: fine-loamy, mixed, superactive, mesic Ultic Haploxeralfs of granitic

153 origin with thick, >5 cm O horizons (Rasmussen et al., 2005). Soil temperature and
154 volumetric water content were measured continuously at multiple depths in the top meter
155 in nearby (within 50 m) control plots of a soil warming experiment as described in Hicks
156 Pries et al. (2017b).

157 *Soil Characterization*

158 Three soil pits within 120 m of each other were dug to a depth of 100 cm in
159 August 2013. Coarse (>2 mm) and fine (<2 mm) roots were sampled from 0-10, 10-20,
160 20-30, 30-50, 50-80, and 80-100 cm depths within 25 x 25 cm quadrats while the soil pits
161 were dug. We characterized the profiles according to procedures outlined in the NRCS
162 Soil Manual (2012), delineating the depth of each genetic horizon. Bulk density was
163 sampled in the center of each soil horizon (5-6 horizons per pit) using a small handheld
164 hammer corer (5.35 cm in diameter by 10 cm long; Table S1). For all other soil analyses,
165 we collected 10 cm long increments of soil that were 4 cm wide by 4 cm into the pit face
166 from 0 to 100 cm for a total of 10 samples per pit. Soil samples were stored at 4°C in
167 plastic bags. Within two days, we processed the soil samples in the lab. Bulk density
168 samples were sorted to remove roots and rocks, weighed, and a 10-15 g subsample was
169 dried at 105°C until it maintained a constant weight to determine moisture content. The
170 soil sampled in 10 cm increments similarly had roots and rocks removed and was then
171 dried at 50°C for 4 days. A subsample of the dried soil was ground with stainless steel
172 balls in stainless steel canisters on a roller mill for 48 hours and if necessary, on a Spex
173 mill, and then analyzed by Elemental Analyzer-Isotope Ratio Mass Spectrometer (EA-
174 IRMS; IsoPrime 100 IRMS in line with a Vario micro cube EA, Isoprime, United
175 Kingdom) for %C, %N, $\delta^{13}C$, and $\delta^{15}N$. For all depths and analyses, there are three reps,
176 one per soil pit.

177 Microbial biomass C (MBC) was measured using a modified fumigation-
178 extraction procedure (Joergensen and Mueller, 1996; Vance et al., 1987). In brief,
179 duplicate 20 g field-moist samples were either extracted immediately with 80 ml of 0.05
180 M K_2SO_4 for an hour and then filtered through a Whatman #1 filter or extracted similarly
181 after fumigation in a chloroform atmosphere for five days to ensure chloroform reached
182 all soil pores. Extracts were diluted and run for TC on a Shimadzu TOC-V Analyzer
183 (Shimadzu North America, Columbia, MD). MBC was calculated as the difference
184 between TC in fumigated and non-fumigated samples, divided by a correction factor of
185 0.45 (Beck et al., 1997). Soils were sampled for MBC in June 2014, 2015, and 2016, as
186 well as in December 2014 from 10-20, 50-60, and 80-90 cm.
187 Benzene polycarboxylic acids (BPCA) were used as a proxy for pyrogenic C in
188 the soil samples and were measured according to Wiedemeier et al. (2016, 2013). The
189 BCPA yields were directly reported as BPCA-C (%SOC), without the use of a conversion
190 factor. Performance and high reproducibility were checked by measuring samples in
191 triplicates and simultaneously running external standards (Wiedemeier et al., 2016).
192 *Root Decomposition*
193 To grow ^{13}C-labeled roots, in 2013, *Avena fatua* seeds were sown in a 50:50
194 mixture of vermiculite and sand and grown in a greenhouse within an airtight chamber. A
195 Li-Cor 840 (LiCor, Nebraska) and datalogger (CR800, Campbell Scientific) monitored
196 the air inside the chamber and opened a solenoid valve to let in CO_2 when concentrations
197 dropped below 390 ppm. About every 4 days the source of CO_2 was switched between
198 tanks of unlabeled CO_2 and 10 atom% $^{13}CO_2$ (Cambridge Isotope Laboratories, Inc.,
199 Massachusetts, USA). The plants were watered on an 'as needed' basis. We harvested the
200 *Avena* after it went to seed by cutting off the stems and then shaking the roots loose from

201 the potting mixture and rinsing the roots in water. The *Avena* material was then dried for
202 a week at 40°C. Three subsamples of the roots were ground and analyzed for %C and ^{13}C
203 using a Thermo Delta V Plus isotope ratio mass spectrometer interfaced to a Costech
204 ECS 4010 CHNSO analyzer (EA-IRMS) at the Center for Isotope Geochemistry at
205 Lawrence Berkeley National Laboratory. The %C and ^{13}C were 46.3% and 4255‰,
206 respectively (Castanha et al., 2018).
207 We added 0.5 g of dried *Avena* fine root (<2 mm diameter) at each of three depths
208 (15, 55, and 95 cm) to three walls of each soil pit (n=3) in November 2013, so that each
209 pit would have three sets of roots, one for each of the collection times. The depths
210 corresponded to the AB, Bt, and BC genetic horizons, respectively. This amount of C was
211 equivalent to 2%, 8%, and 11% of the native SOC pool at 15, 55, and 95 cm,
212 respectively. *Avena fatua* is an annual grass; its roots were used as a common substrate so
213 that its decomposition could be compared across studies (e.g., Castanha et al., 2018).
214 These roots (C:N=39) were likely more decomposable than the coniferous roots native to
215 the site (Silver and Miya, 2001). At each depth, the roots were added to a 10.2 cm
216 diameter circular area. Each area had twenty, 4 cm deep (into the pit wall) holes that were
217 created by a 2.5 mm diameter metal stake in which we inserted 4 cm long bunches of fine
218 roots (≈0.025 mg). We inserted the roots this way to minimize soil structure disturbance.
219 We marked where the roots were placed using tent stakes below the insertion area and
220 placed mesh (fiberglass window screen) over each side of the pit before filling the pit
221 back in. The mesh allowed us to find the sides of the pits when we had to dig them out
222 again to collect the incubated roots.

223 The first collection of the root litter took place in June 2014 (6 months) and
224 subsequent collections occurred in November 2014 (12 months) and June 2016 (30
225 months). To collect the root litter and associated soil, we used a capped and sharpened
226 PVC collar (10 cm in diameter by 10 cm deep) that we hammered into the side of the pit
227 around where the roots had been inserted. We used another PVC sampler to collect
228 control soil from the same depth and side of the pit about 20 cm away from the root
229 sample. After collection, the pits were refilled. The samples were stored in plastic bags at
230 4°C. In the laboratory, samples were sieved through a 2-mm mesh into coarse particulate
231 (CPOM, > 2 mm, included identifiable root litter pieces) and bulk soil (<2 mm) fractions,
232 weighed, freeze-dried, and re-weighed to determine moisture content. Dried subsamples
233 were ground and analyzed for %C, %N, and $\delta^{13}C$ using the aforementioned EA-IRMS.
234 The bulk soil fraction was further separated by density into free light (fLF)
235 occluded light (oLF), and dense fractions (DF) using a 1.7 g ml^{-1} sodium polytungstate
236 solution and methods refined in our lab (Bird and Torn, 2006; Swanston et al., 2005). We
237 added 50 ml of 1.7 g ml^{-1} of low C/N sodium polytungstate solution (SPT_0, TC-Tungsten
238 Compounds Inc., Grub am Forst, Germany) to 20 g of air-dried soil in a conical based
239 polycarbonate centrifuge bottle. The bottle was gently inverted several times to ensure
240 that all soil was in contact with the SPT solution. Any remaining soil particles were
241 rinsed from lids and rims of centrifuge bottles and the samples were left to equilibrate on
242 the bench top for 1hr to ensure maximum separation between light and mineral associated
243 fractions before being centrifuged in a swinging bucket rotor for 1 hour at 3500*rpm* (4710
244 x g) and 25°C. The fLF (<1.7 g ml^{-1}) was vacuum aspirated from the centrifuge bottle,
245 filtered through a 0.8 μm polycarbonate filter (Nucleopore Track-Etch, Whatman), and

246 rinsed with Nanopure reagent grade water (18.2 MΩ-cm) until the filtrate was the density
247 of water. Aggregates were physically disrupted by mixing the remaining sample in SPT
248 solution using a benchtop mixer (G3U05R, Lightnin) at 75% power for 1 minute
249 followed by sonication (Branson 450) in an ice bath at maximum output and 70% pulse
250 for 1.5 min for a total energy input of 100 J ml^{-1}. The samples were equilibrated for one
251 hour on the bench top and subsequently centrifuged for 1 hour at 3500rpm (4710 x g),
252 allowed to settle overnight followed by vacuum aspiration of the floating material, the
253 oLF, which was then filtered and rinsed following the same procedure as for the fLF.
254 The remaining sample, the DF, was rinsed of residual SPT with Nanopure water until the
255 supernatant was the density of water. A flocculant consisting of 30 ml of 1 M $CaCl_2$ in 3
256 ml of 1 M HCl was added to samples prior to rinsing to prevent dissolution of metal
257 oxide minerals and ensure complete recovery of sample material. All fractions were dried
258 at 105°C, weighed, ground, and analyzed for %C, %N, and $\delta^{13}C$ by EA-IRMS. Average
259 recoveries were 101% for mass and 88% for C.
260 The amount of root litter-derived C recovered in each fraction was calculated by
261 multiplying the fraction of litter-derived C by the total amount of C in that fraction. The
262 proportion of litter-derived C in each fraction was calculated using a simple mixing
263 model:

264 $$I_{AS} = f_{soil} * I_{CS} + f_{root} * I_{root}$$
265 $$1 = f_{soil} + f_{root}$$
266
267 where *I* is the isotopic content ($\delta^{13}C$), subscript *AS* denotes the value of the soil, fraction,
268 or phospholipid fatty acid (PLFA) that had root litter added to it, *CS* denotes the control
269 value from the corresponding pit, depth, timepoint (except for CPOM, in which we only
270 used timepoint 3 of the controls), and PLFA (where applicable), and *root* denotes the

value of the labeled root litter. f_{soil} is the proportion of C derived from native soil and f_{root} is the proportion of C derived from the labeled litter. The percent of litter-derived C remaining was calculated as the amount of recovered C divided by the total amount added to the soil at the beginning of the experiment multiplied by 100.

Phospholipid Fatty Acid Analysis

In order to identify soil microbial communities and their assimilation of the labeled root substrate by depth, a PLFA extraction was performed on freeze-dried soils using previously described procedures (Bird et al., 2011; White and Ringelberg, 1998). Approximately 10 g of soil was analyzed for the 15 and 55 cm depths, and 12 g for 95 cm in order to compensate for lower microbial biomass at depth (Fierer et al., 2003). Recovery from samples was determined using di-19:0 PC (1, 2-Dinonadecanoylsn-Glycero-3-Phosphocoline, Avanti Polar Lipids, Alabaster, AL, USA), which was added to the soils before the extraction. Additionally, a 10:0 fatty acid methyl ester standard (FAME; ethyl decanoate, Sigma-Aldrich, Inc., St. Louis, MO, USA) was added to samples prior to gas chromatography. The FAMEs were analyzed on a Hewlett Packard (Agilent) 5890 Series II Gas Chromatograph (GC) with a 30 m x 0.32 mm x 1.0 mm ZB-5 column (Phenomenex, Inc., Torrance, CA, USA) connected via a Europa ORCHID on-line combustion interfaced to an IsoPrime 100 Isotope Ratio Mass Spectrometer (IRMS, IsoPrime, Cheadle, UK). Bacterial fatty acid standards were used to identify peaks (MIDI, Newark, DE).

PLFA biomarkers were used to quantify the relative abundances of different microbial groups. Thirteen PLFA biomarkers were assigned to six categories: Gram-positive bacteria (15:0i, 15:0a, 17:0i, 17:0a), Gram-negative bacteria (16:1u7, 18:1u7),

295 fungi (18:2u6,9, 18:1u9), actinobacteria (16:010Me, 18:010Me), protozoa (20:4u6,9),
296 cyclopropyl bacterial (17:0cyc, 19:0cyc) (Zelles 1999, Zogg et al. 1997). Unassigned
297 PLFAs (14:0, 14:0i, 15:0, 15:1i, 16:0, 16:0 12Me, 16:0i, 16:1 2OH,
298 16:1i, 16:1w5c, 16:1w9c, 17:0, 17:0 10Me, 17:1w8c, 18:0, 18:1w5c, 18:1w7c 11Me,
299 20:0, 20:1w9c, i17:1) were included in total PLFA yields and community analyses (Bird et
300 al., 2011). The IRMS was used to determine the $\delta^{13}C$ so the proportion of PLFA-C
301 incorporating the ^{13}C-labeled root substrate could be identified using the mixing model
302 described above. The preference for added root or native soil C was quantified by
303 subtracting the mole percent of native soil-derived C from the mole percent of labeled
304 root-derived C in each PLFA.
305 *CORPSE Model*
306 The Carbon Organisms Rhizosphere and Protection in the Soil Environment
307 (CORPSE) model simulates soil organic matter formation and decomposition with a
308 focus on microbial and mineral interactions (Fig 1; Sulman et al., 2014). See the
309 Supplemental Information for full model equations and parameters and the code used to
310 run the model. Organic substrates are divided into three chemically-defined classes
311 representing rapidly-decomposing compounds (such as sugars and cellulose), slowly-
312 decomposing compounds (such as lignin), and microbial necromass. Decomposition of
313 these substrates is controlled by a dynamic microbial biomass pool. Rapidly-
314 decomposing compounds have high maximum decomposition rates and microbial carbon
315 use efficiencies, and as a result they stimulate microbial growth, allowing the model to
316 simulate acceleration of decomposition through inputs of fresh organic matter and root
317 exudates (priming effects). Organic substrates exist in either unprotected or protected

forms, with protected organic matter temporarily inaccessible to microbial decomposition. Organic matter is transferred between unprotected and protected pools at fixed rates, with microbial necromass having a higher protection rate than other substrates. The model structure allows organic matter to be divided into isotopically labeled and unlabeled fractions to facilitate comparison with isotope tracking measurements but does not simulate any isotopic fractionation via biochemical processes.

We simulated decomposition of isotope-labeled root litter by initializing the model with 0.5 mg of root mass, which was assumed to contain 25% rapidly-decomposing compounds and 75% slowly-decomposing compounds in line with previous CORPSE simulations (e.g., Sulman et al., 2017). We drove the model for the 15, 55, and 95 cm depths by interpolating measured profiles of soil temperature and moisture to the appropriate depths. In addition, each depth received root exudate inputs calculated based on the observed profile of living fine roots. Root exudation rate was calculated based on measured fine root (< 2 mm) biomass at each depth, following estimates of exudation per fine root biomass from Phillips et al. (2011) and assuming that exudation rates were relatively higher nearer the surface to account for other sources of fresh carbon such as leaching from the litter layer. The resulting input rates per unit root biomass were 26.2 mg C g root^{-1} year^{-1} at 15 cm depth and 6.5 mg C g root^{-1} year^{-1} at 55 and 95 cm depths, and input rates per unit soil volume were 0.13 mg C cm^{-3} year^{-1} at 15 cm depth, 0.0094 mg C cm^{-3} year^{-1} at 55 cm depth, and 0.0082 mg C cm^{-3} year^{-1} at 95 cm depth. To capture the range of potential decomposition environments due to the high spatial heterogeneity at depth, we also ran an additional simulation at 95 cm depth without any root exudate inputs.

341 *Statistical Analyses*
342
343 We analyzed the measured data using linear models in R (R Development Core
344 Team, 2017) with the continuous variables (depth and time), as the main effects and a
345 depth by time interaction. For analysis of root recovery in fractions, fraction—bulk and
346 particulate or free light, occluded light, and dense—was an additional fixed effect. For
347 PLFA analyses, PLFA or biomarker and treatment (control or labeled) were additional
348 fixed effects. We used Akaike's Information Criteria (AIC)-based model selection to
349 determine whether variance structures or a random effect, in this case soil pit, improved
350 the models following Zuur et al. (2009). We also used stepwise model reduction and AIC
351 to determine which fixed effects and interactions were significant in the models. We
352 tested all 2-way and 3-way interactions. When interactions among continuous main
353 effects were significant, we set up multiple comparisons using the lstrends command in
354 the lsmeans package (Lenth, 2016). For each fraction (where applicable), we tested depth
355 slopes with time set at 6, 12, and 30 months and time slopes with depth set at 15, 55, and
356 95 cm; we used the multivariate *t* distribution to test for significance at $\alpha<0.05$ taking into
357 account the number of multiple comparisons. When only categorical main effects were
358 significant, we performed contrasts with a Tukey adjustment in lsmeans with the
359 continuous main effects held at their mean values. We also fit an exponential decay
360 model to the data using the nls package in R and chose the best model based on AIC
361 (Tables S1 and S2).

362 **Results**

363 *Soil Characterization*

We characterized how SOC, root biomass, microbial biomass, and climate (temperature and moisture) changed with depth. These soils stored 16.6±1.7 kg C m^{-2} in the top meter of mineral soil, with 45% of this SOC stored below 20 cm. Carbon concentrations decreased from 8.3% in the top 10 cm to an average of 0.37% below 60 cm (Fig. 2a). Nitrogen concentrations also decreased, from 0.3% at the surface to 0.01% below 60 cm. The C:N ratio decreased from 28 in the top 10 cm to 23.6 at 60-70 cm before increasing to 34 at 90-100 cm (Fig. 2b). $\delta^{13}C$ became enriched from 0-10 cm to around 60-70 cm before it became more depleted towards 90-100 cm (Fig. 2c). Pyrogenic C was most concentrated at 15 cm and had similar, low concentrations at 55 and 95 cm (Fig. 2d). Fine root (<2 mm) density declined steeply in the top 40 cm while coarse root (>2 mm) density peaked around 40 cm (Fig. 2e). The proportion of SOC in the three density fractions differed significantly ($p<0.0001$). About half of SOC was in the dense fraction and 23-36% in the free light fraction (Fig. 2f); however, the distribution of SOC among the fractions did not differ significantly by depth (depth x fraction interaction, $p=0.11$). Microbial biomass declined more linearly with soil depth than did SOC (Fig. 2g). The ratio of microbial biomass C to SOC was ≈10 mg g^{-1} at both 15 and 95 cm but was 22 mg g^{-1} at 55 cm. Soil bulk density increased with depth while pH generally decreased from 6.2 at the 5 cm to 5.6 at 75 cm before increasing to 6.5 at 95 cm (Tables S1 and S2). Soil temperature and volumetric water content averaged 11°C and 26% over the 2.5-year experiment, respectively, and the averages did not differ among depths (Fig. 2h and 2i). However, surface soils experienced a more temporally variable climate than deeper soils (Fig. S1).

Root Decomposition

Loss of root litter C during the first 6 months was similar across all depths with 62% of applied root C remaining (Fig. 3). However, after 30 months, root C loss was significantly faster at 15 cm than at 55 cm and significantly faster at 55 cm than at 95 cm with 25, 40, and 62% of applied root C remaining, respectively. In the regression model, these differences in retention with depth resulted in a significant depth x time interaction ($p=0.017$, $f=6.7$, $df=1$). Recoveries after 6 and 12 months were similar across depths but differed across depths after 30 months ($p<0.05$). We also fit an exponential decay model to the data (Fig. S2, Table S3). The best fit model, based on AIC, was a double exponential decay model with the parameter controlling the decay rate of the slow pool controlled by depth (Table S4). With this model, the estimated turnover times were about 0.3 years for the fast-decaying pool and 3, 6-9, and 7-10,000 years for the slow-decaying pool at 15, 55, and 95 cm, respectively. The wide range in values at 95 cm was due to fitting the model with and without the outlier from the 30-month sampling, which showed zero mass loss after 12 months, and reflected the spatial heterogeneity of soils at depth (Table S3).

At each sampling point, the amount of applied root C recovered in the bulk soil fraction (<2 mm) was significantly smaller than the amount recovered in the coarse particulate fraction (i.e., as identifiable root pieces, $p=0.009$; Fig. 4). The loss of the coarse particulate fraction drove the decrease in the amount of total root C recovered over time at 15 and 55 cm (time x fraction interaction, $p=0.08$), but the coarse fraction did not decrease over time at 95 cm (time x depth interaction, $p=0.02$). As a result, there was more root C recovered in the coarse particulate fraction at 95 cm than at 15 or 55 cm, but similar amounts of root C recovered in the bulk fraction at 30 months (depth x fraction

410 interaction, p=0.009). Within the bulk fraction, the percent of root C recovered among the
411 three density fractions did not differ by depth (p=0.58) or time (6 and 30 months only,
412 p=0.97) but did differ significantly by fraction (p<0.0001; Fig. 5). Among the density
413 fractions, none of the two-way interactions with time, depth, and fraction were significant
414 (p>0.25).

415 *Phospholipid Fatty Acids*
416
417 There were no significant differences in the relative abundances of PLFA's
418 between the control soils and soils to which labeled roots had been added (p=0.63,
419 f=0.23, df=1). Looking at just the control soil, there were significant changes in certain
420 biomarker abundances with depth (depth x biomarker interaction, p=0.0001; Fig. 6a). The
421 abundances of the fungal biomarker, 18:1w9c, and the Gram-negative biomarker,
422 18:1w7c, both decreased significantly with depth. The two actinomycetes biomarkers,
423 16:0 10 Me and 18:0 10Me, both increased significantly with depth. We investigated
424 whether the different microbial groups preferred the native soil C or added root C (Fig.
425 6b). The actinomycetes biomarkers showed a preference for the native soil C, while the
426 fungal and Gram-negative biomarkers showed a preference for the added root C. The
427 Gram-positive biomarkers did not show a preference. In general, the microbes whose
428 relative abundances increased with depth showed a preference for native SOC, while the
429 microbes whose relative abundances decreased with depth showed a preference for added
430 root C.

431 *CORPSE model simulations*

432 Results from the CORPSE model simulations agreed with observations showing
433 that initial rates of root C loss were similar across depths in the first year of

434 decomposition but diverged afterwards (Fig. 7a). At 30 months, decomposition was
435 projected to be fastest at 15 cm and slowest at 95 cm, where root exudate inputs were
436 lower. Similar patterns across time and depth were projected in the amount of root C
437 remaining in the unprotected pool, which is similar to the coarse particulate plus the free
438 light fraction measured in the experiment (Fig. 7b). In contrast, the amount of root C
439 remaining in the protected pool, similar to the dense fractions, reached an asymptote at
440 around 5% between 6 and 10 months and was similar across depths (Fig. 7c). The model
441 results matched the observed patterns of remaining root C in the total, unprotected
442 (coarse and fine particulate), and protected (dense, mineral-associated), with two
443 exceptions. First, differences in total root C remaining among depths at 30 months were
444 greater in the experiment than were predicted by the model, and second, the initial
445 decomposition rate and subsequent loss of C from the unprotected pool and gain of C in
446 the protected pool were faster in the experiment. We also compared turnover times
447 estimated from CORPSE simulations with the double exponential decay model fitted to
448 the experimental data (Tables S1 and S3). Initial turnover times estimated for the first 6
449 months by CORPSE were 1.3-1.4 years versus 0.28-0.32 years for the fast-decaying pool
450 of the exponential decay model fit to the experimental observations (Table S3, S5 and
451 Fig. S3). Longer-term turnover times were more similar, with 3.6 and 3.8 years at 15 cm
452 and 8.6 and 9.1 years at 55 cm, estimated by CORPSE and the exponential decay model,
453 respectively. Both the CORPSE and exponential decay model estimated wide ranges in
454 longer-term turnover times at 95 cm: ranging from 10.8 to 82.8 years, with and without
455 exudates in CORPSE, and from 7 to 10,000 years, depending on the inclusion of the 30-
456 month outlier from the data.

Discussion

Other than decreasing SOC concentrations, the biggest changes with depth in the soil profile were biotic—both microbial and root biomass decreased. In contrast to other soil profiles (Kögel-Knabner et al., 2008; Schrumpf et al., 2013), however, the proportion of SOC that was mineral-associated did not increase with depth. Instead, the proportion of SOC that was mineral-associated (i.e., DF) versus fine particulate (i.e., fLF) remained constant with depth. The average microclimate at all depths was also similar during the experiment, although temperature and moisture extremes were greatest at 15 cm depth. We tested the effect of different soil temperature and moisture regimes among depths with CORPSE, by running the model with the actual soil temperature and moisture at each depth and holding all other parameters constant. This simulation showed only very minor decomposition differences among depths (Fig. S1). Oxygen also did not differ much among depths and was above 16% at all depths (data not shown). Based on the soil profile data we collected, it seems that any differences in root litter decomposition among depths were likely biotically driven.

Mineralization of root litter C was similar across depths over the first 12 months, matching the results of the few previous studies that examined root decomposition across multiple depths in situ (Bird and Torn, 2006; Sanaullah et al., 2011; Solly et al., 2015). However, after 30 months, mineralization differed among depths, as it did after 10 years in the decomposition experiment started by Bird and Torn (Hicks Pries et al., 2017a). Similar initial root mineralization suggests that the microbial potential to decompose the fast-decaying portion of litter inputs is similar at all depths. Over time in situ, however, the litter is fragmented and mineralized more slowly at depth, suggesting that microbial

capacity at depth becomes limited as the pool of labile litter C and N are depleted. This was consistent with CORPSE model results, in which initial microbial decay was supported by the labile content of root inputs at all depths but decay rates diverged once this initial pulse of labile C was depleted.

The similar initial root mineralization rates indicate that the conditions for rapid microbial degradation of labile, accessible SOC exists at all depths. Fungi and Gram-negative bacteria preferentially assimilated the added root-derived C relative to native SOC. Despite greater relative abundances of fungi and Gram-negative bacteria towards the soil surface, the shift in microbial communities with depth did not result in a difference in initial decomposition. Their abundances likely reflected the profile of native SOC substrates, as the addition of root litter did not change microbial communities at any depth. Microbial biomass per gram SOC was similar at the surface and at 95 cm, and the aforementioned microbial groups that preferred the root litter were present at all depths. Furthermore, the microbes experienced similar microclimates at all depths during the first six months of decomposition with average temperatures of 8.2-8.6°C and average volumetric water contents of 25-28%.

Slower longer-term root mineralization in deeper soil was not due to root C becoming associated with mineral surfaces. The amount of root-derived C associated with minerals was constant across depths and did not change between 6 and 30 months, remaining at about 5%. In a similar coniferous forest, 5% of C from root or needle litter was also mineral-associated in the A horizon after 10 years (Hicks Pries et al., 2017a). This potential upper limit on the amount of litter C that could become mineral-associated at this site could indicate C saturation (Castellano et al., 2015; Stewart et al., 2008), but

503 the specific mechanisms leading to C saturation are unclear given the patchy distribution
504 of OM on minerals and potential for organo-organo interactions (Vogel et al., 2014).
505 Moreover, it is unlikely that the soil at 55 or 95 cm is C saturated given the paucity of soil
506 C (<0.7%) at those depths. A more plausible explanation for similar amounts of root C
507 becoming mineral-associated is related to the Microbial Efficiency-Matrix Stabilization
508 hypothesis (MEMS; Cotrufo et al., 2015, 2013). MEMS states that the more labile
509 portions of litter become mineral-associated because those portions are most efficiently
510 (i.e., have a higher anabolism:catabolism ratio) converted into microbial residues that can
511 then sorb to minerals. Our experiment's 5% limit on the amount of root litter becoming
512 mineral-associated may depend on characteristics inherent to the litter itself and therefore
513 is the same across depths. The speed at which the root-derived C became mineral-
514 associated in our study—5% within 6 months—supports earlier research hypothesizing
515 that initial decomposition products become sorbed to minerals (Cotrufo et al., 2015;
516 Rumpel et al., 2010; Swanston et al., 2005). The CORPSE model is consistent with the
517 MEMS hypothesis via its assumption that microbial necromass forms the bulk of
518 protected C, and the model successfully captured the observed pattern of 5% of root C
519 becoming "protected" (CORPSE does not explicitly distinguish protection mechanisms
520 between occluded and mineral-associated pools) at all depths.
521 The main differences in root litter decomposition among depths occurred in the
522 coarse particulate fraction, which was the only size or density fraction that significantly
523 differed in the amount of root-derived C among depths after 30 months. The roots in the
524 coarse particulate fraction, which were still identifiable roots, were likely increasingly
525 resistant to decomposition with depth for several reasons. There was a shift in microbial

526 communities with fewer fungal biomarkers extracted at depth. Saprotrophic fungi
527 preferentially decompose the structural components of roots such as cellulose and lignin
528 (Baldrian, 2017; Dashtban et al., 2010), which may in turn allow bacterial decomposers
529 to access the interior root tissue. The fungal and Gram-negative biomarkers that preferred
530 the added root substrate were less abundant at depth, which might affect longer term
531 decomposition in ways that did not affect initial decomposition. However, a previous
532 study using ^{13}C-PLFA found decreasing fungal enrichment in ^{13}C from added root litter
533 in an annual grassland as decomposition progressed, implying the fungal role was in
534 initial decomposition (Herman et al., 2012).
535 The amount of root exudates in our soils likely decreases with depth due to
536 declining fine root biomass. Thus, while differences in microbial communities may result
537 in different root decomposition rates, there is a causality dilemma in that differences in
538 root exudation can drive microbial community differences and may thus be the proximal
539 cause of the observed decomposition differences. Root exudates and associated changes
540 in the rhizosphere soil can increase SOC mineralization rates—by 59% on average
541 according to a recent meta-analysis (Huo et al., 2017). To investigate whether a priming
542 effect could have caused the differences in root decomposition with depth, we compared
543 our observations to simulations using the CORPSE model wherein we decreased root
544 exudate inputs with depth. Priming in the model did not affect initial decomposition rates
545 but did affect longer-term decomposition rates, which matched the observations well in
546 terms of total recovery, recovery in various pools, and both initial and long-term litter C
547 turnover times. In particular, rapid initial mineralization at all depths was supported by
548 labile C present in the root inputs, while long-term mineralization rates diverged once

549 these labile compounds were depleted. This is consistent with the hypothesis that
550 continuing fresh inputs of labile C support faster decomposition in surface soils compared
551 to subsoils. In surface soils, microbes can use the energy provided by exudates to
552 synthesize enzymes needed to decompose the remaining root-derived compounds that
553 have higher energetic barriers to decay (Blagodatskaya and Kuzyakov, 2008). According
554 to this hypothesis, breaking down root-derived OM remaining after the initial phase of
555 decomposition in deeper soils is not energetically favorable given the low availability of
556 labile compounds, so decomposition rates are very slow. Positive priming effects have
557 been induced in incubations of subsoils by adding glucose or organic acids and the
558 priming effects were greater in subsoil than in surface soil, implying labile substrates are
559 more limiting to microbial activity in subsoils (Fontaine et al., 2007; Heitkötter et al.,
560 2017; Tian et al., 2016).
561 While the CORPSE model does well explaining the trends in our experimental
562 data, it does not fully recreate the magnitude of differences in later stages of root
563 decomposition among depths. There are likely other mechanisms driving faster
564 decomposition at the surface than at depth that were not included in CORPSE model.
565 One mechanism is nitrogen limitation of microbial activity in deeper soils (Heitkötter et
566 al., 2017), which may be likely in our soils where the C:N ratio is greater at depth relative
567 to surface soil. The effects of N on decomposition rates are highly variable, but generally
568 positive for low N environments (Knorr et al., 2005). Nitrogen addition increases
569 cellulose-degrading enzyme activities (Keeler et al., 2009) and fungal decomposition of
570 low nitrogen, lignin-rich litter (Allison et al., 2009; Jiang et al., 2014). Decomposition at
571 depth can be limited by both nitrogen and labile substrates; a recent incubation

572 experiment found that adding nitrogen to subsoils (30-60 cm) increased the priming
573 response to added glucose by 18% (Tian et al., 2016). Recent work incorporating N
574 cycling into the CORPSE model (Sulman et al., 2017) will allow us to investigate the role
575 of N limitation on subsoil SOC decomposition in future analyses.

576 Another potential mechanism for slower decomposition of roots in the coarse
577 particulate fraction is the lack of soil fauna at depth that can increase litter surface area
578 via fragmentation (Knowles et al., 2016) and the delivery of labile substrates by creating
579 preferential flow paths. The abundance of bioturbation agents like arthropods generally
580 declines steeply with depth (Jiménez and Decaëns, 2000; Petersen and Luxton, 1982).
581 While there are no earthworms in our soils and faunal abundance was not measured in
582 this experiment, the potential role of bioturbation agents in differentiating litter
583 decomposition processes among depths warrants future study.

584 Slower root litter decomposition rates may contribute to the older age of native
585 SOC with depth (Hicks Pries et al., 2017b). The effect of slower root litter decomposition
586 with depth is shown in estimates of coarse POC turnover time, which increased from 24
587 years at 15 cm to 126 years at 95 cm (Table S6). If microbial processing is needed for
588 litter SOC to interact with minerals, mineral interactions will not occur if SOC is stuck in
589 the particulate pool, which may explain why the proportion of SOC that was mineral-
590 associated did not increase with depth in our soils. Furthermore, the old age of mineral-
591 associated SOC with depth may partly be due to the time it takes for coarse particulate
592 matter to be decomposed and become mineral-associated.

593 The decrease in root decomposition with depth may also explain the increase in
594 C:N ratios and depletion in $\delta^{13}C$ that occurred around 60 cm in our soils. In general,

595 microbial processing of SOC causes C:N ratios to decrease with depth (Rumpel and
596 Kögel-Knabner, 2011), as more C has been respired, and $\delta^{13}C$ to become enriched with
597 depth, as a result of catabolic carboxylation reactions (Ehleringer et al., 2000). However,
598 in our soil, the trend in C:N and $\delta^{13}C$ reverses below 60 cm. Pyrogenic C can have very
599 high C:N ratios (>100; Rajkovich et al., 2012) but the proportion of SOC that was
600 pyrogenic decreased with depth in our soils. Therefore, higher C:N ratios and more
601 depleted $\delta^{13}C$ at depth were likely due to deep SOC being less microbially-processed and
602 more closely resembling the original plant inputs. At depth, the likely source of SOC
603 inputs is roots (Rasse et al., 2005; Schmidt et al., 2011); in the absence of bioturbation,
604 very little leaf and needle-derived organic matter deposited at the surface will move down
605 the soil profile (Hicks Pries et al., 2017a). It remains to be seen whether slower
606 particulate OM decomposition with depth occurs in other soils.
607 Our results indicate that slower root litter decomposition may contribute to longer
608 residence times of SOC with depth, but that slower root litter decomposition may not be
609 driven by increased organo-mineral associations. Our model results suggest that root litter
610 decomposition may be limited by labile C availability. Thus, particulate SOC at depth
611 could be vulnerable to priming-induced increases in decomposition, if the rate of fresh
612 substrates reaching deep soils increases. Thus, a proportion of deep SOC may be
613 vulnerable to global-change-induced losses if increased precipitation leads to enhanced
614 leaching and transport of DOC from the surface litter. On the other hand, increased root
615 production at depth, if the roots are not actively exuding substrates (Tückmantel et al.,
616 2017), would promote deep SOC storage.

617 **Literature Cited**
618

619 Allison, S.D., LeBauer, D.S., Ofrecio, M.R., Reyes, R., Ta, A.-M., Tran, T.M., 2009. Low
620 levels of nitrogen addition stimulate decomposition by boreal forest fungi.
621 Soil Biology and Biochemistry 41, 293–302.
622 Angst, G., Kögel-Knabner, I., Kirfel, K., Hertel, D., Mueller, C.W., 2016. Spatial
623 distribution and chemical composition of soil organic matter fractions in
624 rhizosphere and non-rhizosphere soil under European beech (Fagus
625 sylvatica L.). Geoderma 264, 179–187. doi:10.1016/j.geoderma.2015.10.016
626 Baldrian, P., 2017. Microbial activity and the dynamics of ecosystem processes in
627 forest soils. Current Opinion in Microbiology, SI: 37 Environmental
628 microbiology 37, 128–134. doi:10.1016/j.mib.2017.06.008
629 Beck, T., Joergensen, R.G., Kandeler, E., Makeschin, F., Nuss, E., Oberholzer, H.R.,
630 Scheu, S., 1997. An inter-laboratory comparison of ten different ways of
631 measuring soil microbial biomass C. Soil Biology and Biochemistry 29, 1023–
632 1032.
633 Bird, J.A., Herman, D.J., Firestone, M.K., 2011. Rhizosphere priming of soil organic
634 matter by bacterial groups in a grassland soil. Soil Biology and Biochemistry
635 43, 718–725.
636 Bird, J.A., Torn, M.S., 2006. Fine roots vs. needles: a comparison of 13C and 15N
637 dynamics in a ponderosa pine forest soil. Biogeochemistry 79, 361–382.
638 Blagodatskaya, E., Kuzyakov, Y., 2008. Mechanisms of real and apparent priming
639 effects and their dependence on soil microbial biomass and community
640 structure: critical review. Biology and Fertility of Soils 45, 115–131.
641 doi:10.1007/s00374-008-0334-y
642 Castanha, C., Zhu, B., Pries, C.E.H., Georgiou, K., Torn, M.S., 2018. The effects of
643 heating, rhizosphere, and depth on root litter decomposition are mediated by
644 soil moisture. Biogeochemistry 137, 267–279.
645 Castellano, M.J., Mueller, K.E., Olk, D.C., Sawyer, J.E., Six, J., 2015. Integrating plant
646 litter quality, soil organic matter stabilization, and the carbon saturation
647 concept. Global Change Biology 21, 3200–3209.
648 Cotrufo, M.F., Soong, J.L., Horton, A.J., Campbell, E.E., Haddix, M.L., Wall, D.H., Parton,
649 W.J., 2015. Formation of soil organic matter via biochemical and physical
650 pathways of litter mass loss. Nature Geoscience 8, 776–779.
651 doi:10.1038/ngeo2520
652 Cotrufo, M.F., Wallenstein, M.D., Boot, C.M., Denef, K., Paul, E., 2013. The Microbial
653 Efficiency-Matrix Stabilization (MEMS) framework integrates plant litter
654 decomposition with soil organic matter stabilization: do labile plant inputs
655 form stable soil organic matter? Global Change Biology 19, 988–995.
656 doi:10.1111/gcb.12113
657 Dashtban, M., Schraft, H., Syed, T.A., Qin, W., 2010. Fungal biodegradation and
658 enzymatic modification of lignin. International Journal of Biochemistry and
659 Molecular Biology 1, 36–50.
660 Ehleringer, J.R., Buchmann, N., Flanagan, L.B., 2000. Carbon isotope ratios in
661 belowground carbon cycle processes. Ecological Applications 10, 412–422.
662 Eilers, K.G., Debenport, S., Anderson, S., Fierer, N., 2012. Digging deeper to find
663 unique microbial communities: The strong effect of depth on the structure of

664 bacterial and archaeal communities in soil. Soil Biology and Biochemistry 50,
665 58–65. doi:10.1016/j.soilbio.2012.03.011
666 Fierer, N., Schimel, J.P., Holden, P.A., 2003. Variations in microbial community
667 composition through two soil depth profiles. Soil Biology and Biochemistry
668 35, 167–176. doi:10.1016/S0038-0717(02)00251-1
669 Fontaine, S., Barot, S., Barré, P., Bdioui, N., Mary, B., Rumpel, C., 2007. Stability of
670 organic carbon in deep soil layers controlled by fresh carbon supply. Nature
671 450, 277–280.
672 Gabriel, C.-E., Kellman, L., 2014. Investigating the role of moisture as an
673 environmental constraint in the decomposition of shallow and deep mineral
674 soil organic matter of a temperate coniferous soil. Soil Biology and
675 Biochemistry 68, 373–384. doi:10.1016/j.soilbio.2013.10.009
676 Gill, R.A., Burke, I.C., 2002. Influence of soil depth on the decomposition of
677 <Emphasis Type="Italic">Bouteloua gracilis</Emphasis> roots in the
678 shortgrass steppe. Plant and Soil 241, 233–242.
679 doi:10.1023/A:1016146805542
680 Gillabel, J., Cebrian-Lopez, B., Six, J., Merckx, R., 2010. Experimental evidence for the
681 attenuating effect of SOM protection on temperature sensitivity of SOM
682 decomposition. Global Change Biology 16, 2789–2798. doi:10.1111/j.1365-
683 2486.2009.02132.x
684 Gleixner, G., 2013. Soil organic matter dynamics: a biological perspective derived
685 from the use of compound-specific isotopes studies. Ecological Research 28,
686 683–695. doi:10.1007/s11284-012-1022-9
687 Heinze, S., Ludwig, B., Piepho, H.-P., Mikutta, R., Don, A., Wordell-Dietrich, P.,
688 Helfrich, M., Hertel, D., Leuschner, C., Kirfel, K., Kandeler, E., Preusser, S.,
689 Guggenberger, G., Leinemann, T., Marschner, B., 2018. Factors controlling the
690 variability of organic matter in the top- and subsoil of a sandy Dystric
691 Cambisol under beech forest. Geoderma 311, 37–44.
692 doi:10.1016/j.geoderma.2017.09.028
693 Heitkötter, J., Heinze, S., Marschner, B., 2017. Relevance of substrate quality and
694 nutrients for microbial C-turnover in top- and subsoil of a Dystric Cambisol.
695 Geoderma 302, 89–99. doi:10.1016/j.geoderma.2017.04.029
696 Herman, D.J., Firestone, M.K., Nuccio, E., Hodge, A., 2012. Interactions between an
697 arbuscular mycorrhizal fungus and a soil microbial community mediating
698 litter decomposition. FEMS Microbiology Ecology 80, 236–247.
699 Hicks Pries, C.E., Bird, J.A., Castanha, C., Hatton, P.-J., Torn, M.S., 2017a. Long term
700 decomposition: the influence of litter type and soil horizon on retention of
701 plant carbon and nitrogen in soils. Biogeochemistry 134, 5–16.
702 Hicks Pries, C.E., Castanha, C., Porras, R.C., Torn, M.S., 2017b. The whole-soil carbon
703 flux in response to warming. Science 355, 1420–1423.
704 Huo, C., Luo, Y., Cheng, W., 2017. Rhizosphere priming effect: A meta-analysis. Soil
705 Biology and Biochemistry 111, 78–84. doi:10.1016/j.soilbio.2017.04.003
706 Jenkinson, D.S., Coleman, K., 2008. The turnover of organic carbon in subsoils. Part 2.
707 Modelling carbon turnover. European Journal of Soil Science 59, 400–413.
708 doi:10.1111/j.1365-2389.2008.01026.x

709 Jiang, X., Cao, L., Zhang, R., Yan, L., Mao, Y., Yang, Y., 2014. Effects of nitrogen addition
710 and litter properties on litter decomposition and enzyme activities of
711 individual fungi. Applied Soil Ecology 80, 108–115.
712 doi:10.1016/j.apsoil.2014.04.002
713 Jiménez, J.J., Decaëns, T., 2000. Vertical distribution of earthworms in grassland soils
714 of the Colombian Llanos. Biology and Fertility of Soils 32, 463–473.
715 doi:10.1007/s003740000277
716 Jobbágy, E.G., Jackson, R.B., 2000. The vertical distribution of soil organic carbon and
717 its relation to climate and vegetation. Ecological Applications 10, 423–436.
718 Joergensen, R.G., Mueller, T., 1996. The fumigation-extraction method to estimate
719 soil microbial biomass: Calibration of the kEN value. Soil Biology and
720 Biochemistry 28, 33–37. doi:10.1016/0038-0717(95)00101-8
721 Karhu, K., Hilasvuori, E., Fritze, H., Biasi, C., Nykänen, H., Liski, J., Vanhala, P.,
722 Heinonsalo, J., Pumpanen, J., 2016. Priming effect increases with depth in a
723 boreal forest soil. Soil Biology and Biochemistry 99, 104–107.
724 doi:10.1016/j.soilbio.2016.05.001
725 Keeler, B.L., Hobbie, S.E., Kellogg, L.E., 2009. Effects of long-term nitrogen addition
726 on microbial enzyme activity in eight forested and grassland sites:
727 implications for litter and soil organic matter decomposition. Ecosystems 12,
728 1–15.
729 Knorr, M., Frey, S.D., Curtis, P.S., 2005. Nitrogen additions and litter decomposition:
730 A meta-analysis. Ecology 86, 3252–3257.
731 Knowles, M.E., Ross, D.S., Görres, J.H., 2016. Effect of the endogeic earthworm
732 Aporrectodea tuberculata on aggregation and carbon redistribution in
733 uninvaded forest soil columns. Soil Biology and Biochemistry 100, 192–200.
734 doi:10.1016/j.soilbio.2016.06.016
735 Kögel-Knabner, I., Guggenberger, G., Kleber, M., Kandeler, E., Kalbitz, K., Scheu, S.,
736 Eusterhues, K., Leinweber, P., 2008. Organo-mineral associations in
737 temperate soils: Integrating biology, mineralogy, and organic matter
738 chemistry. Journal of Plant Nutrition and Soil Science 171, 61–82.
739 doi:10.1002/jpln.200700048
740 Koven, C.D., Riley, W.J., Stern, A., 2013. Analysis of permafrost thermal dynamics and
741 response to climate change in the CMIP5 Earth System Models. Journal of
742 Climate 26, 1877–1900.
743 Kramer, C., Gleixner, G., 2008. Soil organic matter in soil depth profiles: distinct
744 carbon preferences of microbial groups during carbon transformation. Soil
745 Biology and Biochemistry 40, 425–433.
746 Kuzyakov, Y., 2010. Priming effects: Interactions between living and dead organic
747 matter. Soil Biology and Biochemistry 42, 1363–1371.
748 doi:10.1016/j.soilbio.2010.04.003
749 Lavelle, P., 1988. Earthworm activities and the soil system. Biology and Fertility of
750 Soils 6, 237–251.
751 Lavelle, P., Decaëns, T., Aubert, M., Barot, S., Blouin, M., Bureau, F., Margerie, P., Mora,
752 P., Rossi, J.-P., 2006. Soil invertebrates and ecosystem services. European
753 Journal of Soil Biology 42, S3–S15.

754 Lenth, R.V., 2016. Least-Squares Means: The R Package lsmeans | Lenth | Journal of
755 Statistical Software. doi:10.18637/jss.v069.i01
756 Mathieu, J.A., Hatté, C., Balesdent, J., Parent, É., 2015. Deep soil carbon dynamics are
757 driven more by soil type than by climate: a worldwide meta-analysis of
758 radiocarbon profiles. Global Change Biology 21, 4278–4292.
759 doi:10.1111/gcb.13012
760 Petersen, H., Luxton, M., 1982. A Comparative Analysis of Soil Fauna Populations and
761 Their Role in Decomposition Processes. Oikos 39, 288–388.
762 doi:10.2307/3544689
763 Phillips, R.P., Finzi, A.C., Bernhardt, E.S., 2011. Enhanced root exudation induces
764 microbial feedbacks to N cycling in a pine forest under long-term CO2
765 fumigation. Ecology Letters 14, 187–194.
766 Preusser, S., Marhan, S., Poll, C., Kandeler, E., 2017. Microbial community response to
767 changes in substrate availability and habitat conditions in a reciprocal
768 subsoil transfer experiment. Soil Biology and Biochemistry 105, 138–152.
769 doi:10.1016/j.soilbio.2016.11.021
770 R Development Core Team, 2017. R: A language and environment for statistical
771 computing. R Foundation for Statistical Computing, Vienna, Austria.
772 Rajkovich, S., Enders, A., Hanley, K., Hyland, C., Zimmerman, A.R., Lehmann, J., 2012.
773 Corn growth and nitrogen nutrition after additions of biochars with varying
774 properties to a temperate soil. Biology and Fertility of Soils 48, 271–284.
775 Rasmussen, C., Torn, M.S., Southard, R.J., 2005. Mineral assemblage and aggregates
776 control carbon dynamics in a California conifer forest. Soil Science Society of
777 America Journal 69, 1711–1721.
778 Rasse, D.P., Rumpel, C., Dignac, M.-F., 2005. Is soil carbon mostly root carbon?
779 Mechanisms for a specific stabilisation. Plant and Soil 269, 341–356.
780 doi:10.1007/s11104-004-0907-y
781 Rumpel, C., Eusterhues, K., Kögel-Knabner, I., 2010. Non-cellulosic neutral sugar
782 contribution to mineral associated organic matter in top-and subsoil
783 horizons of two acid forest soils. Soil Biology and Biochemistry 42, 379–382.
784 Rumpel, C., Kögel-Knabner, I., 2011. Deep soil organic matter—a key but poorly
785 understood component of terrestrial C cycle. Plant and Soil 338, 143–158.
786 Rumpel, C., Kögel-Knabner, I., Bruhn, F., 2002. Vertical distribution, age, and
787 chemical composition of organic carbon in two forest soils of different
788 pedogenesis. Organic Geochemistry 33, 1131–1142.
789 Salomé, C., Nunan, N., Pouteau, V., Lerch, T.Z., Chenu, C., 2010. Carbon dynamics in
790 topsoil and in subsoil may be controlled by different regulatory mechanisms.
791 Global Change Biology 16, 416–426. doi:10.1111/j.1365-2486.2009.01884.x
792 Sanaullah, M., Chabbi, A., Leifeld, J., Bardoux, G., Billou, D., Rumpel, C., 2011.
793 Decomposition and stabilization of root litter in top-and subsoil horizons:
794 what is the difference? Plant and Soil 338, 127–141.
795 Schmidt, M.W., Torn, M.S., Abiven, S., Dittmar, T., Guggenberger, G., Janssens, I.A.,
796 Kleber, M., Kögel-Knabner, I., Lehmann, J., Manning, D.A., others, 2011.
797 Persistence of soil organic matter as an ecosystem property. Nature 478, 49–
798 56.

799 Schrumpf, M., Kaiser, K., Guggenberger, G., Persson, T., Kögel-Knabner, I., Schulze, E.-
800 D., 2013. Storage and stability of organic carbon in soils as related to depth,
801 occlusion within aggregates, and attachment to minerals. Biogeosciences 10,
802 1675–1691.
803 Silver, W.L., Miya, R.K., 2001. Global patterns in root decomposition: comparisons of
804 climate and litter quality effects. Oecologia 129, 407–419.
805 doi:10.1007/s004420100740
806 Six, J., Bossuyt, H., Degryze, S., Denef, K., 2004. A history of research on the link
807 between (micro) aggregates, soil biota, and soil organic matter dynamics. Soil
808 and Tillage Research 79, 7–31.
809 Soil Science Division Staff, 2012. Soil survey manual, USDA Handbook 18.
810 Government Printing Office, Washington, D.C.
811 Solly, E.F., Schöning, I., Herold, N., Trumbore, S.E., Schrumpf, M., 2015. No depth-
812 dependence of fine root litter decomposition in temperate beech forest soils.
813 Plant and Soil 393, 273–282. doi:10.1007/s11104-015-2492-7
814 Stewart, C.E., Paustian, K., Conant, R.T., Plante, A.F., Six, J., 2008. Soil carbon
815 saturation: evaluation and corroboration by long-term incubations. Soil
816 Biology and Biochemistry 40, 1741–1750.
817 Sulman, B.N., Brzostek, E.R., Medici, C., Shevliakova, E., Menge, D.N.L., Phillips, R.P.,
818 2017. Feedbacks between plant N demand and rhizosphere priming depend
819 on type of mycorrhizal association. Ecology Letters 20, 1043–1053.
820 doi:10.1111/ele.12802
821 Sulman, B.N., Phillips, R.P., Oishi, A.C., Shevliakova, E., Pacala, S.W., 2014. Microbe-
822 driven turnover offsets mineral-mediated storage of soil carbon under
823 elevated CO 2. Nature Climate Change 4, 1099.
824 Swanston, C.W., Torn, M.S., Hanson, P.J., Southon, J.R., Garten, C.T., Hanlon, E.M.,
825 Ganio, L., 2005. Initial characterization of processes of soil carbon
826 stabilization using forest stand-level radiocarbon enrichment. Geoderma,
827 Mechanisms and regulation of organic matter stabilisation in soils 128, 52–
828 62. doi:10.1016/j.geoderma.2004.12.015
829 Tian, Q., Yang, X., Wang, X., Liao, C., Li, Q., Wang, M., Wu, Y., Liu, F., 2016. Microbial
830 community mediated response of organic carbon mineralization to labile
831 carbon and nitrogen addition in topsoil and subsoil. Biogeochemistry 128,
832 125–139. doi:10.1007/s10533-016-0198-4
833 Tückmantel, T., Leuschner, C., Preusser, S., Kandeler, E., Angst, G., Mueller, C.W.,
834 Meier, I.C., 2017. Root exudation patterns in a beech forest: Dependence on
835 soil depth, root morphology, and environment. Soil Biology and Biochemistry
836 107, 188–197. doi:10.1016/j.soilbio.2017.01.006
837 Vance, E.D., Brookes, P.C., Jenkinson, D.S., 1987. An extraction method for measuring
838 soil microbial biomass C. Soil Biology and Biochemistry 19, 703–707.
839 doi:10.1016/0038-0717(87)90052-6
840 Vogel, C., Mueller, C.W., Höschen, C., Buegger, F., Heister, K., Schulz, S., Schloter, M.,
841 Kögel-Knabner, I., 2014. Submicron structures provide preferential spots for
842 carbon and nitrogen sequestration in soils. Nature Communications 5, 2947.
843 doi:10.1038/ncomms3947

White, D.C., Ringelberg, D.B., 1998. Signature lipid biomarker analysis. Techniques in Microbial Ecology 1, 255–272.
Wiedemeier, D.B., Hilf, M.D., Smittenberg, R.H., Haberle, S.G., Schmidt, M.W., 2013. Improved assessment of pyrogenic carbon quantity and quality in environmental samples by high-performance liquid chromatography. Journal of Chromatography A 1304, 246–250.
Wiedemeier, D.B., Lang, S.Q., Gierga, M., Abiven, S., Bernasconi, S.M., Früh-Green, G.L., Hajdas, I., Hanke, U.M., Hilf, M.D., McIntyre, C.P., Scheider, M.P.W., Smittenberg, R.H., Wacker, L., Wiesenberg, G.L.B., Schmidt, M.W.I., 2016. Characterization, Quantification and Compound-specific Isotopic Analysis of Pyrogenic Carbon Using Benzene Polycarboxylic Acids (BPCA). Journal of Visualized Experiments : JoVE. doi:10.3791/53922
Wordell-Dietrich, P., Don, A., Helfrich, M., 2017. Controlling factors for the stability of subsoil carbon in a Dystric Cambisol. Geoderma, 5th International Symposium on Soil Organic Matter 2015 304, 40–48. doi:10.1016/j.geoderma.2016.08.023
Zuur, A., Ieno, E.N., Walker, N., Saveliev, A.A., Smith, G.M., more, & 2, 2009. Mixed Effects Models and Extensions in Ecology with R, 2009 edition. ed. Springer, New York, NY.

Acknowledgements

This work was supported as part of the Terrestrial Ecosystem Science Program by the Director, Office of Science, Office of Biological and Environmental Research, of the U.S. Department of Energy under Contract No. DE-AC02-05CH11231. We gratefully acknowledge Don Herman for assistance in growing the labeled root litter and for assistance with PLFA analysis at the Firestone Laboratory at UC Berkeley, and the UC Berkeley Center for Forestry Blodgett Forest Research Station for access to and support at the field site.

Figure Captions

Figure 1. Diagram of the CORPSE model applied to different soil depths. Model structure and initial root carbon were identical at each depth, while root exudation rates differed by depth. Red arrows show decomposition-related carbon flows and blue arrows show protection-related carbon flows.

Figure 2. Soil profiles of mean ± SE (n = 3 soil pits) percent carbon (a), C:N ratio (b), $\delta^{13}C$ (c), BPCA as a percent of total SOC (d), root density for coarse and fine roots (e), the proportion of SOC found in dense, free light, and occluded light fractions (f). The bottom row contains mean ± SE microbial biomass (g; via chloroform fumigation over 4 timepoints: June and December 2014, June 2015, and June 2016), mean ± SD (averaged over time to show temporal variability) soil temperature (h), and soil volumetric water (i) content over the course of the experiment (November 2013 through June 2016) from n=3 control plots of an adjacent experiment.

Figure 3. The percent of total applied root C recovered at 15, 55, and 95 cm depths after 6, 12, and 30 months of in situ incubation (mean ± SE, n = 3). The total amount of applied root C recovered decreased significantly with year ($p=0.0017$). There was also a significant depth x month interaction ($p=0.017$) because recoveries after 6 and 12 months were similar across depths but differed across depths after 30 months ($\alpha=0.05$, indicated by asterisk). Furthermore, the slopes of the time trend differed significantly among the three depths ($\alpha=0.05$, represented by letters not shared).

Figure 4. The percent of applied root C recovered in bulk (<2 mm) and coarse particulate (>2 mm) size fractions over 6, 12, and 30 months of incubation within three depths of the soil profile (mean ± SE, n = 3). Asterisks indicate at which depths and for which fraction the declining recovery with time trend was significant and upward carets indicate at which time and for which fraction the depth trend was significant ($\alpha=0.05$).

Figure 5. The percent of applied root C recovered in three density fractions of the bulk soil—dense (>1.7 mg/L), occluded light (<1.7 mg/L) and free light (<1.7 mg/L)—after 6 and 30 months within the soil profile (mean ± SE, n = 3). The amount of root recovered was significantly greater in the dense and free light fractions than in the occluded fraction ($p<0.05$) as indicated by letters not shared.

Figure 6. The relative abundances of a subset of phospholipid fatty acids (PLFAs) associated with microbial biomarkers found at 15, 55, and 95 cm within the control samples (a). The asterisks indicate which PLFA's abundances significantly changed with depth ($p<0.08$ for contrasts, depth x biomarker interaction, $p=0.0001$). The relative amounts of C derived from native soil and C derived from the labeled roots after 6 months in each of the biomarker PLFA's (b). A positive value indicates native C was preferred and negative values indicate the labeled root C was preferred while values around zero indicate no preference.

Figure 7. Results of the CORPSE model (lines) and the experimental observations (mean ± SE, circles) for total root C remaining (a), root C remaining in unprotected pools (b), and root C remaining in protected pools (c). To match the pool structure of the CORPSE model, we assigned the coarse particulate plus the free light fraction from the experiment to the unprotected pool and the dense, mineral-associated fraction from the experiment to the protected pool. The CORPSE model was run twice at 95 cm—once with root exudates proportional to root biomass at that depth and once with no root exudates to demonstrate the range of conditions at depth due to high spatial heterogeneity.

Root exudation

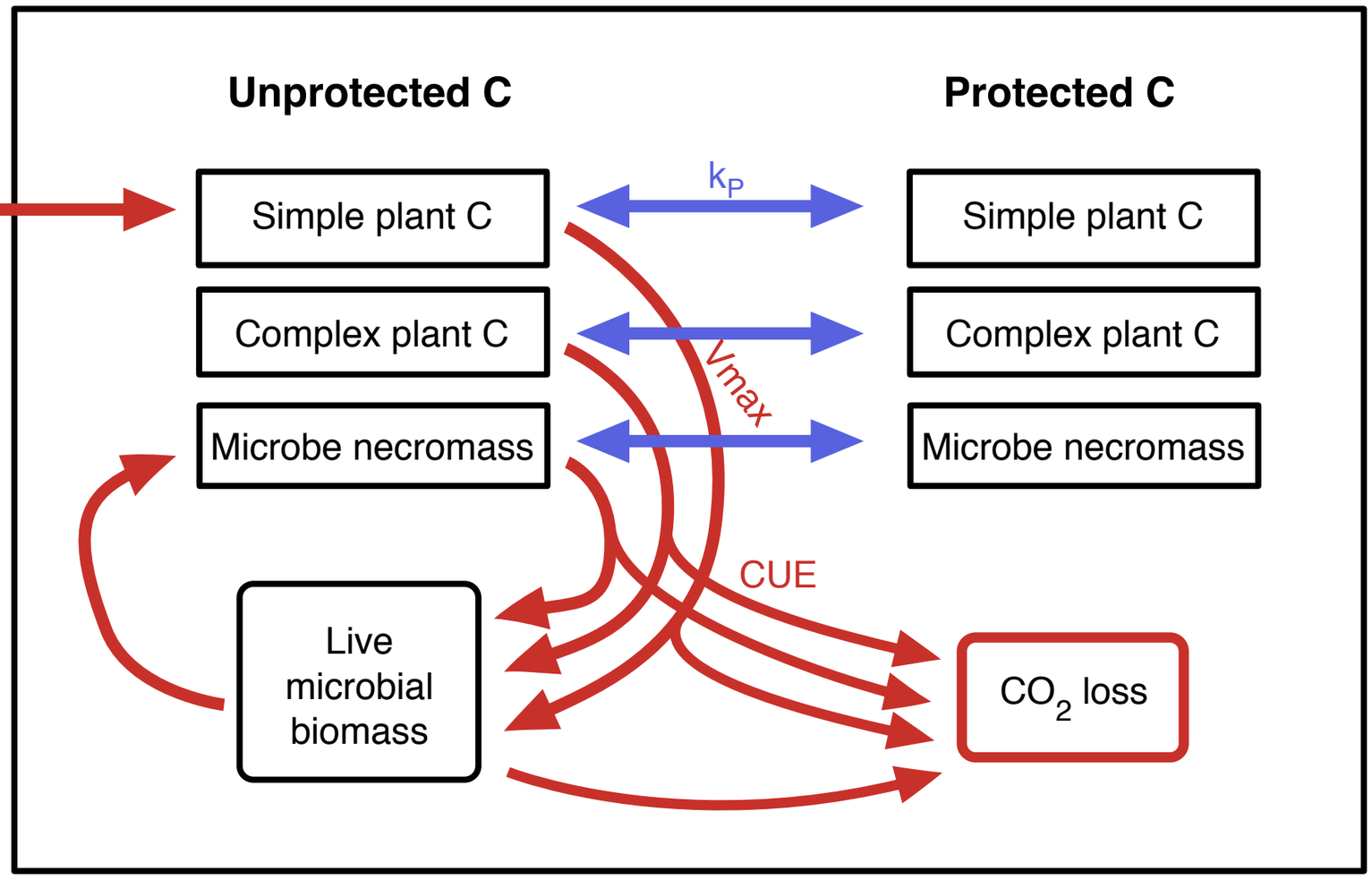

15 cm

Root exudation

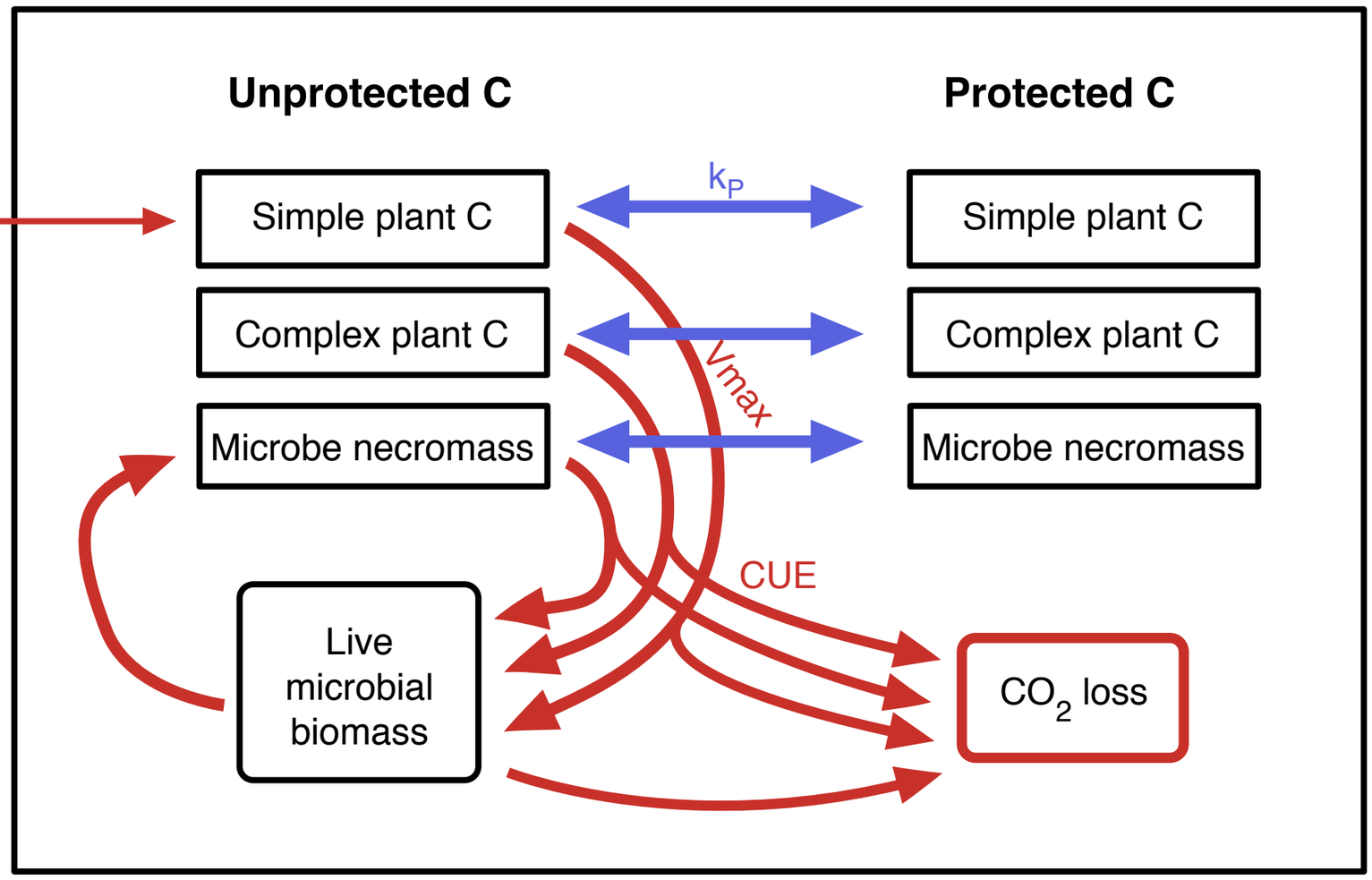

55 cm

Root exudation

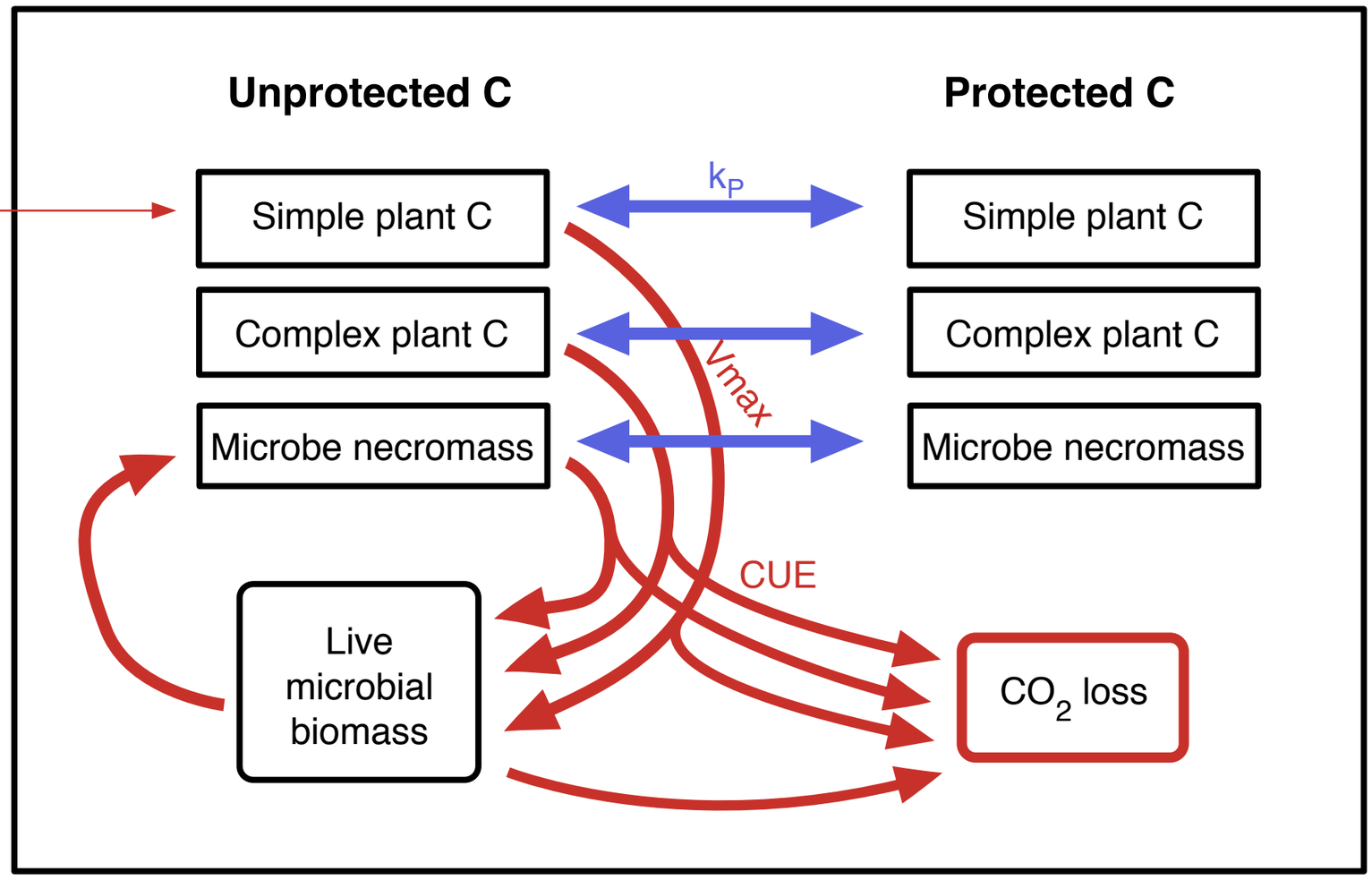

95 cm

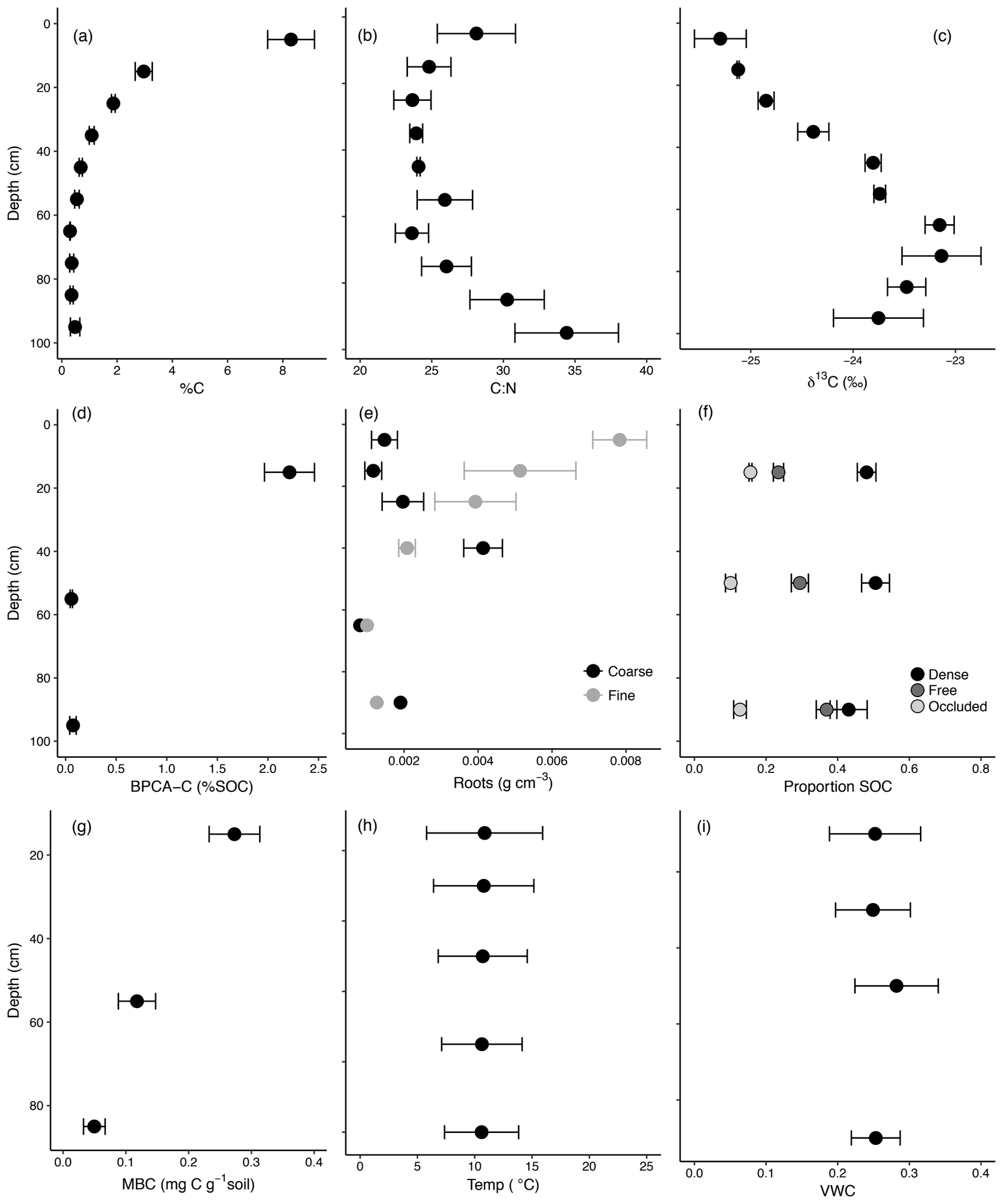
(a)
(b)
(c)
(d)
(e)
(f)
(g)
(h)
(i)
Depth (cm)
%C
C:N
δ13C (‰)
BPCA−C (%SOC)
Roots (g cm−3)
Proportion SOC
MBC (mg C g−1soil)
Temp (°C)
VWC
Coarse
Fine
Dense
Free
Occluded

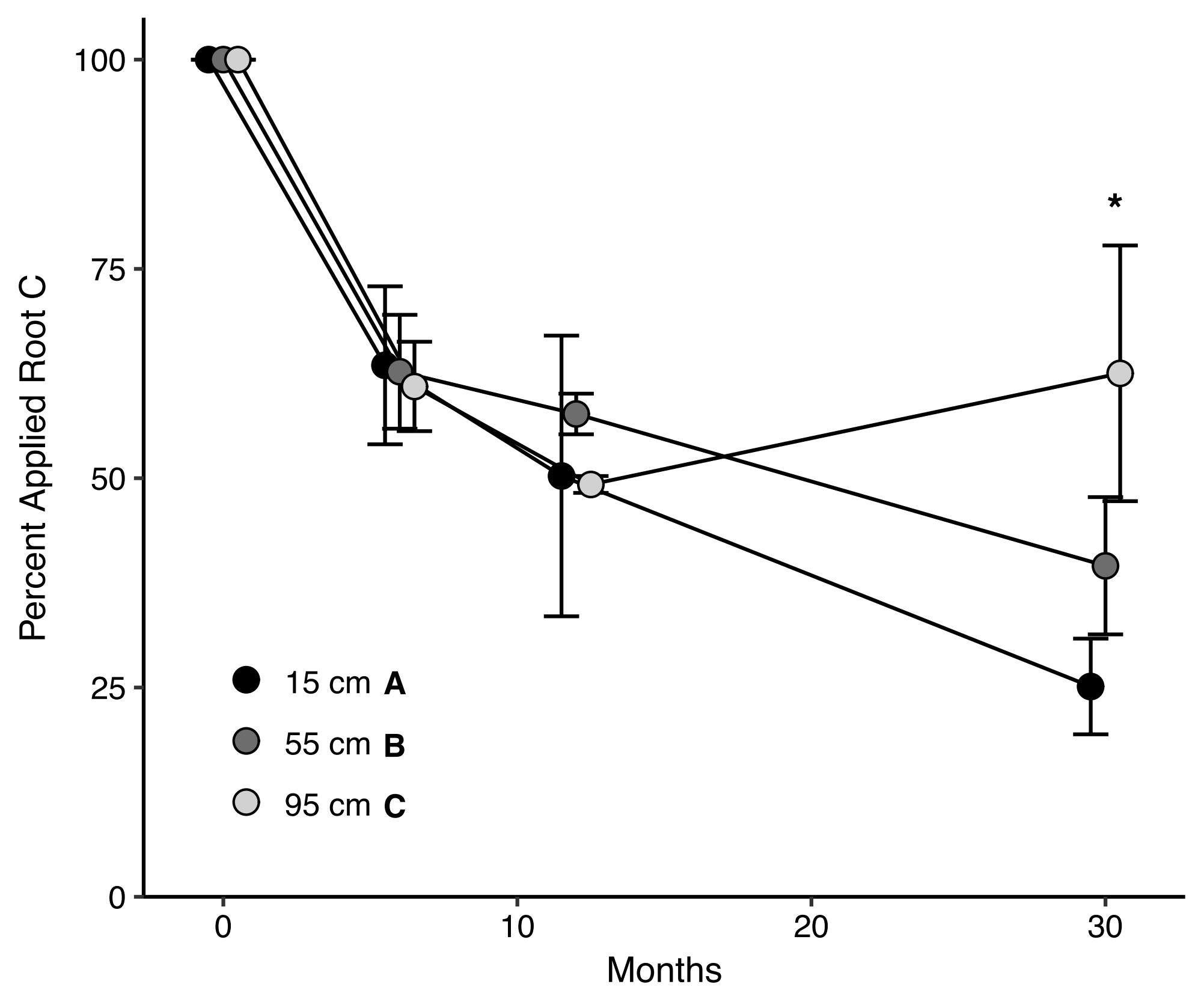
100
75
50
25
0
Percent Applied Root C
0
10
20
30
Months
*
15 cm A
55 cm B
95 cm C

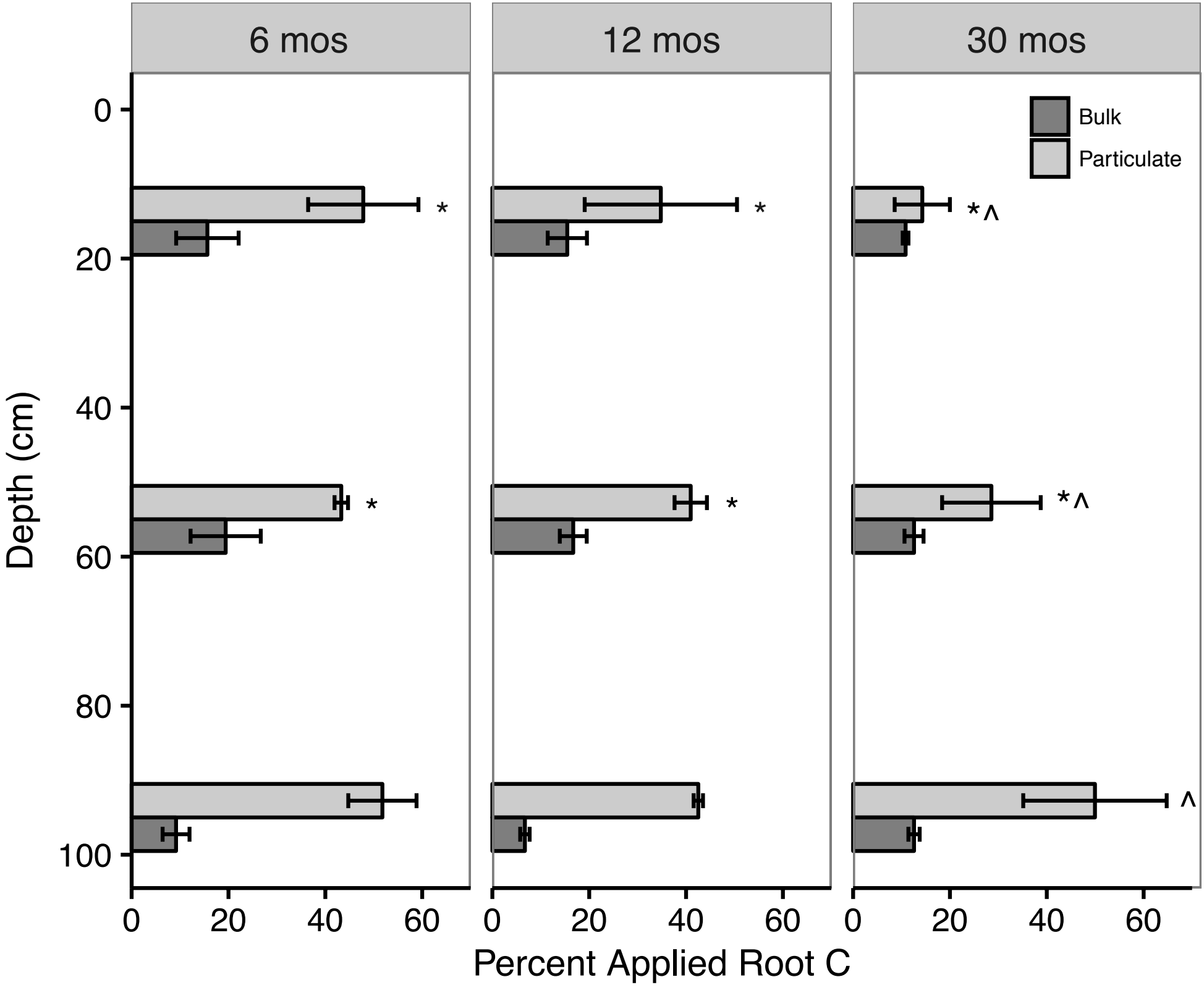
6 mos
12 mos
30 mos
Bulk
Particulate
Depth (cm)
0
20
40
60
80
100
0
20
40
60
Percent Applied Root C
*
*
*
*
*^
*
*^
^

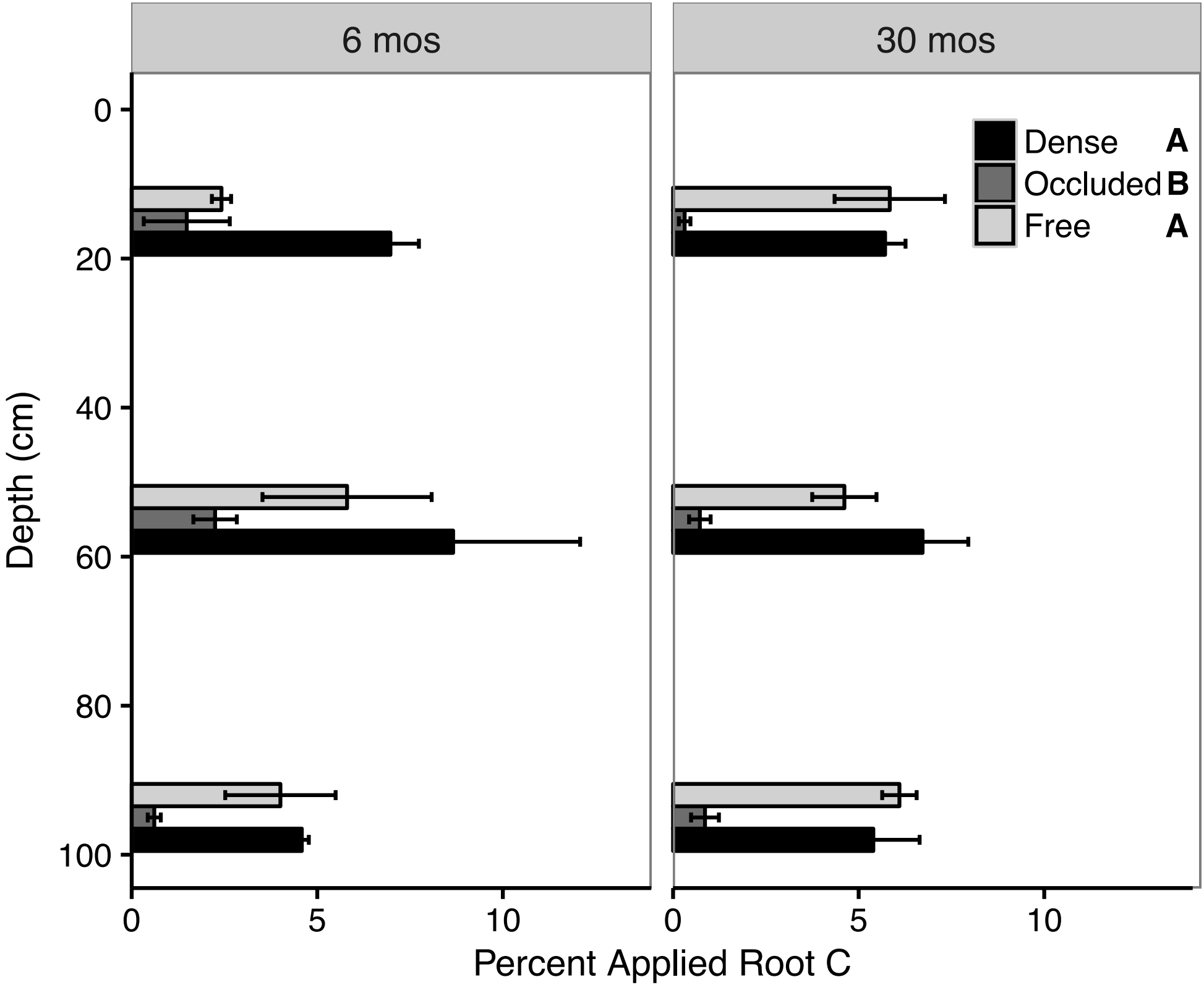
6 mos
30 mos
Dense A
Occluded B
Free A
Depth (cm)
0
20
40
60
80
100
0
5
10
Percent Applied Root C

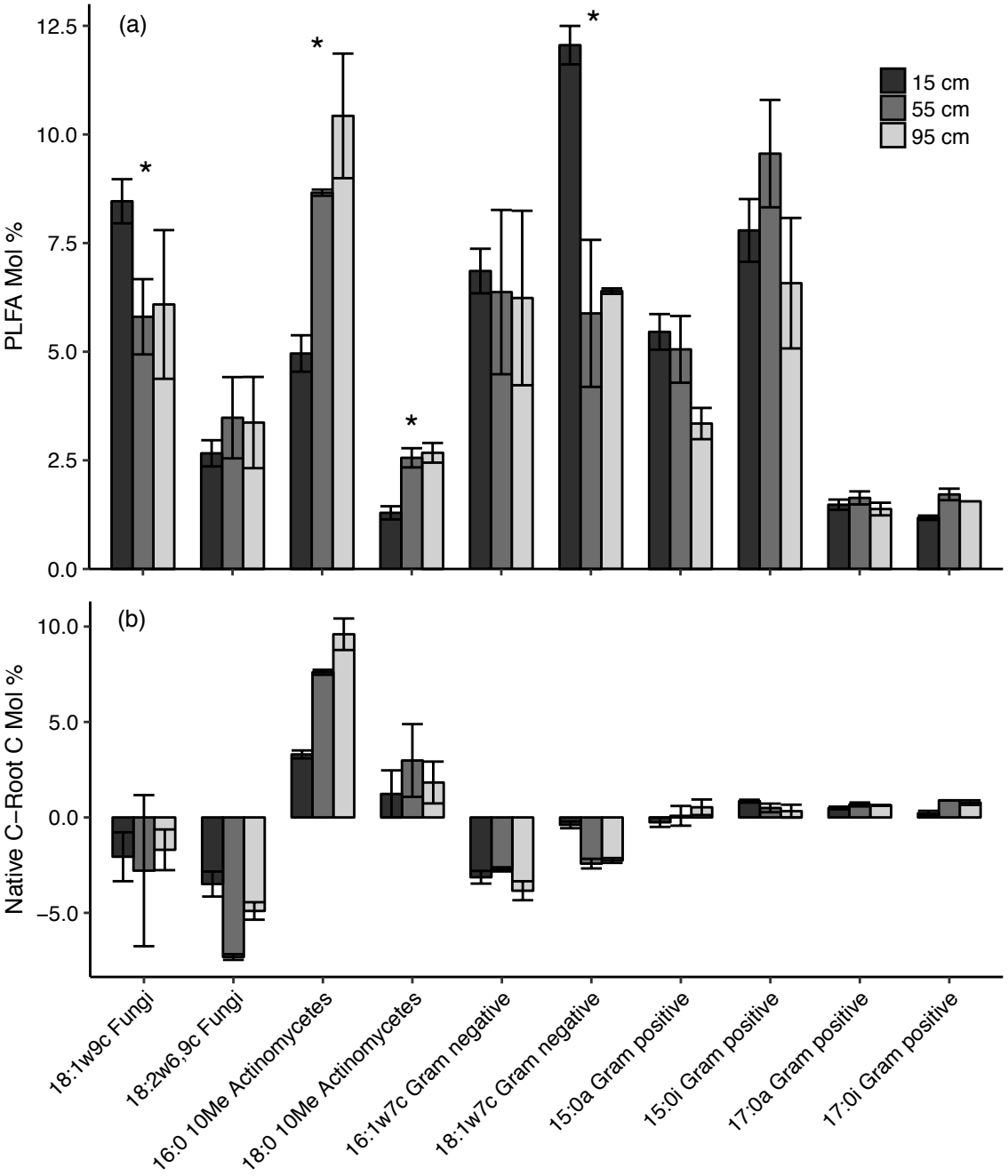
(a)
PLFA Mol %
12.5
10.0
7.5
5.0
2.5
0.0
15 cm
55 cm
95 cm
*
*
*
*
(b)
Native C−Root C Mol %
10.0
5.0
0.0
−5.0
18:1w9c Fungi
18:2w6,9c Fungi
16:0 10Me Actinomycetes
18:0 10Me Actinomycetes
16:1w7c Gram negative
18:1w7c Gram negative
15:0a Gram positive
15:0i Gram positive
17:0a Gram positive
17:0i Gram positive

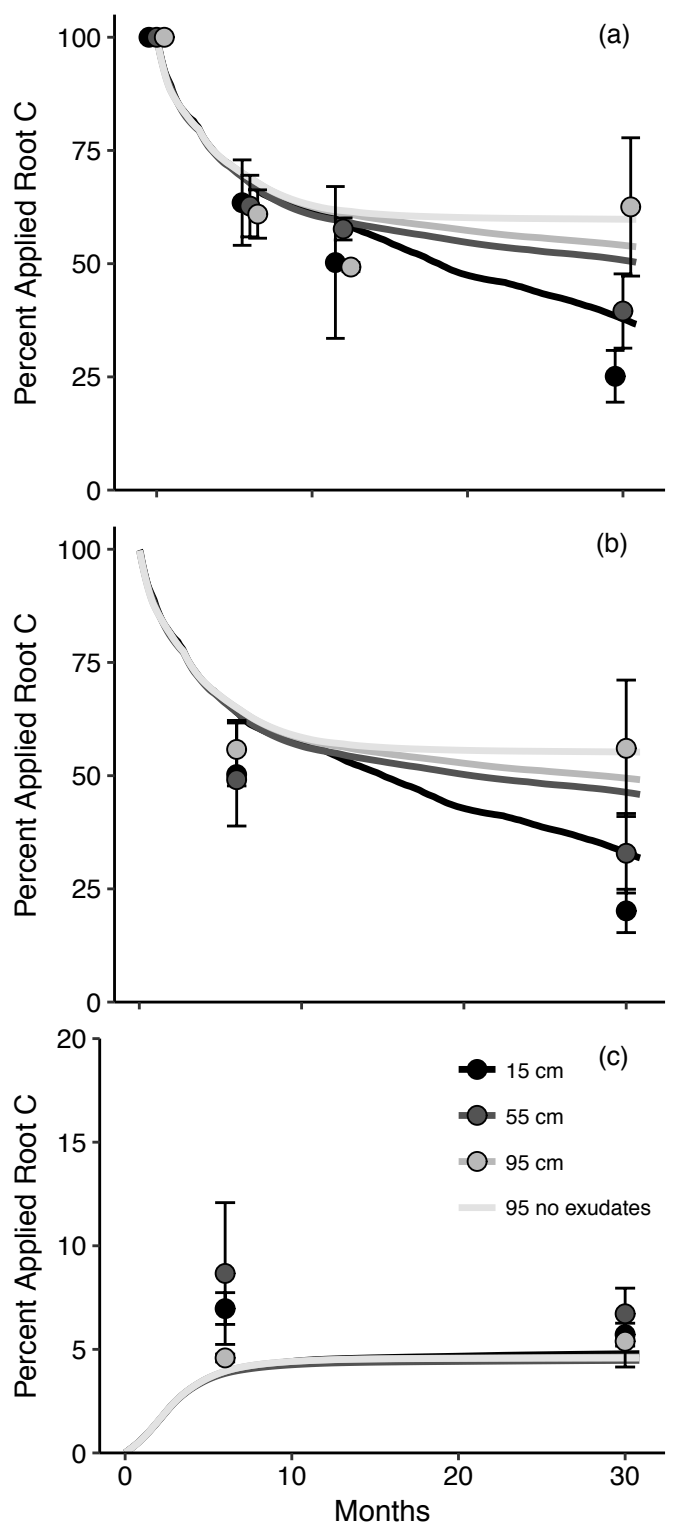
(a)
(b)
(c)
Percent Applied Root C
Months
15 cm
55 cm
95 cm
95 no exudates
0
25
50
75
100
5
10
15
20
30